Accuracy of additively manufactured zirconia four-unit fixed dental prostheses fabricated by stereolithography, digital light processing and material jetting compared with subtractive manufacturing

Jörg Lüchtenborg[1,*]/Evita Willems[2,*], Fei Zhang[2], Christian Wesemann[1], Florian Weiss[1], Julian Nold[1], Jinxing Sun[3,4], Fabien Sandra[5], Jiaming Bai[4], Helen Reveron[5], Jerome Chevalier[5], Benedikt C. Spies[1]

*These authors contributed equally

1) Center for Dental Medicine, Department of Prosthetic Dentistry, Faculty of Medicine, University of Freiburg, Hugstetter Str. 55, 79106 Freiburg, Germany
2) KU Leuven (University of Leuven), Department of Materials Engineering, Kasteelpark Arenberg 44, B-3001 Leuven, Belgium.

   KU Leuven (University of Leuven), Department of Oral Health Sciences, BIOMAT - Biomaterials Research group & UZ Leuven (University Hospitals Leuven), Dentistry, Kapucijnenvoer 7 block a, B-3000 Leuven, Belgium.
3) School of Metallurgy and Materials, University of Birmingham, B15 2TT, UK
4) Shenzhen Key Laboratory for Additive Manufacturing of High-performance Materials， Department of Mechanical and Energy Engineering, Southern University of Science and Technology, Shenzhen, 518055, China
5) Univ Lyon, CNRS, INSA Lyon, UCBL, MATEIS, UMR5510, 69621 Villeurbanne, France

Corresponding author

Jörg Lüchtenborg: joerg.luechtenborg@uniklinik-freiburg.de

Declaration of interest:

none

Abstract

Objective: To evaluate the manufacturing accuracy of zirconia four-unit fixed dental prostheses (FDPs) fabricated by three different additive manufacturing technologies compared with substractive manufacturing.

Methods: A total of 79 zirconia FDPs were produced by three different manufacturing technologies, representing additive (one stereolithography [aSLA] and one material jetting

[aMJ] device, two digital light processing [aDLP1/aDLP2] devices) and subtractive manufacturing (two devices [s1/s2]), the latter serving as references. After printing, additively manufactured FDPs were debound and finally sintered. Subsequently, samples were circumferentially digitized and acquired surface areas were split in three Regions Of Interest (ROIs: inner/outer shell, margin). Design and acquired data were compared for accuracy using an inspection software. Statistical evaluation was performed using the root mean square error (RMSE) and nonparametric Kruskal-Wallis method with post hoc Wilcoxon-Mann-Whitney U tests. Bonferroni correction was applied in case of multiple testing.

Results: Regardless the ROI, significant differences were observed between manufacturing technologies ($P<0.001$). Subtractive manufacturing was the most accurate with no significant difference regarding the material/device (s1/s2, $P>0.054$). Likewise, no statistical difference regarding accurary was found when comparing s2 with aMJ and aSLA in most ROIs ($P>0.085$). In general, mean surface deviation was <50 µm for s1/s2 and aMJ and <100 µm for aSLA and aDLP2. aDLP1 showed surface deviations >100 µm and was the least accurate compared to the other additive/subtractive technologies.

Significance: Additive manufacturing represents a promising set of technologies for the manufacturing of zirconia FDPs, but not yet as accuracte as subtractive manufacturing. Methodogical impact on accuracy within and in between different additive technologies needs to be further investigated.

1. Introduction

In recent years, Additive Manufacturing (AM) has become an integral part of various dental applications. In dental laboratories, models, trays and splints are produced from polymers using various AM technologies [1]. Nowadays, metals, e.g. to be used as frameworks are also processed by means of AM [2]. However, there is an increasing demand for metal-free restorations, resulting in the need for high-strength ceramic materials like oxide ceramics. AM of such ceramics is not yet established in the dental field. In the traditional workflow, various ceramics are available with zirconia being one of the most preferred material [3, 4]. Yttria-stabilized Tetragonal Zirconia Polycrystals containing 3 mol% of Y_2O_3 (often refered as 3Y-TZP) are the most widely used among different zirconia ceramics. They exhibit an excellent combination of fracture toughness (~ 5 $MPa \cdot m^{1/2}$) and flexural strength (~ 1000 MPa) [5]. Stabilizers like yttria are used to retain the tetragonal crystal phase of the zirconia in a metastable state at room temperature. Under the application of mechanical stresses, the tetragonal phase can be transformed to the monoclinic phase, accompanied by a ~4% volume increase which compresses the crack flanks and prevents crack propagation [6].

Nowadays dental zirconia is produced using subtractive manufacturing in a CAD/CAM (computer-aided design and -manufacturing) workflow. Isostatic pressed and pre-sintered blanks with different shades and different flexural strengths are available on the market. Computerized Numerical Controlled (CNC) grinding or milling machines process the restoration from the full material blank, producing a large amount of waste. In contrast, a strong reduction of waste material can be achieved by AM technologies with material only used to build up the part. This can help to reduce the environmental footprint and enable more sustainable manufacturing. AM, as a tool-free production technology, also avoid the problem of wear of the tools used in the CNC machine. Some AM technologies, such as Digital Light Processing (DLP), allow for parallel rather than serial manufacturing, which can lead to significant productivity increase. Finally, all these factors can lead to cost and material's waste reduction in the manufacturing of dental prostheses.

In AM of ceramics, different technologies are considered to have the potential to produce monolithic ceramic dental prostheses. Commercially available technologies include Vat polymerization (Stereolithography/SLA and Digital Ligth Processing/DLP) using light-curable ceramic resin or suspensions as raw materials and Material Jetting (MJ) using ceramic inks [7]. Vat polymerization is the most widely used AM technology for the production of ceramic parts. These processes are based on the local, layerwise photoinitiated polymerization of resins mixed with ceramic particles. The printed part consists of a photopolymerized polymer matrix with embedded ceramic particles. To obtain the final ceramic part, the polymer matrix is burned out in a post-processing step (debinding) and afterwards the part is sintered to obtain a dense monolithic ceramic [8]. Depending on the method, the resin is crosslinked by a laser (SLA) or a digital light projector (DLP) . In SLA technologies, ceramic resins or suspensions are treated by a laser beam that traces photopolymerizable areas, layer by layer, following a sliced 3D-model (STL file). The heigh of a layer typically varies from 10 to 120 μm. After one layer cures, the building platform is lowered or raised in the z-direction (depending on whether the machine uses a "bottom-up" or "top-down" approach) and this process is repeated as many times as necessary. In DLP, since a projector can expose the entire layer at once, the time required for the illumination step is reduced. In the commonly used setup, the projector illuminates the suspension through a window from the bottom. The growing part hangs onto the building platform and for every layer, it is immersed into the suspension (the fabrication of the part takes place "bottom-up"). The resin between part and window is cured and transformed into a solid layer. For the next layer, the part needs to be separated from the window to allow the resin to refill the gap and afterwards these steps are iterated. Material Jetting (MJ) uses inkjet technology, where the material is jetted through a printhead. In polymer material jetting, photopolymers are used, which also allows multimaterial printing. For AM of ceramics, this technology is used by changing the feedstock to an ink that contains ceramic particles. Thousands of nozzles simultaneously jet the building and support material containing inks onto the building platform, generating a part layer by layer. After the support removal, which can be a water-soluble material, the part is debound and sintered to obtain a the ceramic object [9].

When complex geometries are produced by AM technologies, support stuctures are a vital component to any part. The support structures to build up an organic-ceramic device such as a four-unit fixed dental prostheses vary for different AM methods due to the different arrangement of printed-parts at the building platform. Support structures on one hand have to provide sufficient retention of the growing part on the building platform and on the other hand need to withstand the peel force/separation force for hanging SLA or DLP systems, in the so-called "bottom-up" arrangement. In processes where the resin is exposed from above ("top-down"), as the 3DCeram system applied in the present study, there is no peel force/separation force. In these cases, support structures are only necessary for overhanging structures. The components can therefore be arranged on the build platform in such a manner that as few support structures as necessary are required. This avoids damage at the surface and reduces post-processing costs. Nevertheless, in vat polymerization, the support structures are made, due to the process, of the identical material as the desired part. Material Jetting, on the other hand, allows the use of different materials and thus support structures can be printed with a material that can be removed with less effort [10], for example a material soluble in water or other solvents.

Besides reliability of the parts and a competitive manufacturing speed, accuracy is the main challenge for the application of AM fabricated ceramic in dentistry. The accuracy of the manufactured parts is of significant importance for the clinical application. Inaccurate marginal fit can be responsible for plaque retention, micro-leakage and cement breakdown [11, 12]. Poor internal accuracy can increase the thickness of the cement and thus influence the mechanical stability of zirconia-based restorations [13, 14].

Therefore, the aim of the present study was to evaluate the current status of the accuracy of additively compared to subtractive manufactured 3Y-TZP FDPs. For this purpose, FDPs produced with different commercially available additive manufacturing technologies i.e.

stereolithography, digital light processing, and material jetting were compared with the reference standard of subtractively produced FDPs using three-dimensional target/actual comparison.

2. Materials and methods

2.1. Sample preparation

The AM printing process started with a 3D model of a FDP that was converted to the standard triangulation or tessellation language (STL format) before being sliced into layers according to each technology requirements. 79 FDPs, all made of the manufacturers 3Y-TZP material, were produced by different suppliers as follow: Two groups of samples were subtractively manufactured, named s1 (GC, n=16, Zirconia ST, GC, Haasrode, Belgium) and s2 (n=16, priti multidisc ZrO_2 “translucent” Pritidenta, Leinfelden-Echterdingen, Germany); Four groups of samples were produced by three different AM technologies i.e. Stereolithography, named aSLA (n=11, Ceramaker900, 3DCeram, Limoges, France); material jetting, named aMJ (n=16, XJET, Rehovot, Israel) and DLP, named aDLP1 (n=16, 405 nm Prototype DLP-Printer, University of Birmingham, UK) [15] and aDLP2 (n=4, CeraFab System Medical, Lithoz, Vienna, Austria).

Milling of FDPs s1 took 30 min and subsequently the FDPs s1 and s2 were sintered at 1450°C for 6.5h and 2h, respectively.

FDPs of aSLA were printed in 25 μm layers using a commercial 3Y-TZP paste (3D Mix ZrO_2 Zr-P03 grade, 3DCeram) with the use of support structures around the margin and the bottom surface of the pontics that were removed after printing. The pre-set parameters provided by 3DCeram (scraping, hatching and laser power parameters) were employed. The excess, uncured paste was removed using a commercial liquid product (CeraClean, 3DCeram) projected under air pressure. After drying, FDPs were slowly debound in air up to 1150°C and sintered at 1450°C for 2h, following 3DCeram recommendations. No additional post-processing was performed.

The aMJ FDPs were printed using a commercial 3Y-TZP ink (C800 zirconia model dispersion grade 7250001, XJET) using a layer thickness of 10.5 μm. The surrounding support was removed by cleaning the printed fixed dental prostheses in distilled water with a brush. Sintering was performed in air at 1450°C for 2h. Details on the study of aMJ processes on the standard sized bars and disks can be found elsewhere [16].

aDLP1 FDPs were processed using a prototype DLP Printer equipped with a 405 nm wavelength UV light and X/Y plane resolution of 50 μm pixels. 3Y-TZP parts were printed with 25 μm layer thickness. After printing the parts were first cleaned with a mixture of 50 vol.% HDDA and 50 vol.% ethanol in an ultransonic bath to remove any uncured slurry. After debinding the parts were sintered at 1480°C for 2h. No additional postprocessing was performed. Details on the aDLP1 processing on the standard sized bars and disks can be found elsewhere [15]. aDLP2 FDPs were manufactured using a commercial 3Y-TZP slurry (LithaCon 3Y 230, Lithoz) with a layer thickness of 25 μm. The printed FDPs were cleaned to remove the excess slurry. All the 3D-printed FDPs were debound and finally sintered for 2h at 1450°C in air. Further information on the other processes can be found in the literature on SLA [17] and DLP [18-21].

Main characteristics of the 79 FDPs samples are summarized in Table 2

Table 1: Main features of four-unit fixed dental prostheses (FDPs) samples

Sample	**Technology***	**Raw material (3Y-TZP)**	**Number of FDPs (n)**	**Layer thickness (μm)**	**Sintering (°C/h)**
s1	CAM	Zirconia GC ST	16	-	1450/6.5
s2	milling	Zirconia Pritidenta	16	-	1450/2
aSLA	SLA	3DMix Zr-P03 paste	11	25	1450/2
aMJ	MJ	C800 7250001ink	16	10.5	1450/2
aDLP1	DLP	3Y-TZP	16	25	1480/2
aDLP2	DLP	LithaCon 3Y 230 slurry	4	25	1450/2

**CAM:Computed assisted manufacturing; SLA: Stereolithography; DLP: Digital light processing; MJ: Material jetting*

2.2 Sample digitalization and repeatability testing

Initially, four procedures for the light-optical digitalization were tested for the highest repeatability in preliminary trials to evaluate their feasibility. Due to strong reflections, white and tooth-colored monolithic ceramics are difficult to measure. Coating with powders can improve scannability, but manual application of the powder and the associated nonuniform thickness of the coating can cause inaccuracies. Therefore, a powder-free scan approach was preferred. The four different technologies included a non-contact 3D profilometer with stripe light pattern at 25x magnification (VR-52000, Keyence, Osaka, Japan), a light optical 3D coordinate measuring machine (VL-500, Keyence, Osaka, Japan), a confocal laser scanning (TRIOS 4, 3shape, Copenhagen, Denmark) and a dynamic depth scanning technology (Primescan, DentsplySirona, York, USA). Each FDP was digitized five times repeatedly with each technology. The scans of the different technologies were compared with each other using a 3D target/actual comparison and the repeatability was determined. Finally dynamic depth scanning was used for digitizing the FDPs. All 79 FDPs were digitized 360° by an experienced operator under consistent lighting conditions utilizing a single scan, so that it was not necessary to merge several files. Scan data was then saved as standard triangulation of tessellation language (STL) datasets at maximum resolution.

2.3 Dynamic depth scanning: accuracy measurement procedure

Dynamic depth scanning data were subsequently analyzed with the inspection software Geomagic Control X (Geomagic, 3DSystems) using a three-dimensional target/actual comparison. For this purpose, the planning file was first defined as a target and segmented into the three analysis areas -inner shell, margin and outer shell, as shown in Fig. 1. The margin corresponded to a 0.25 mm horizontal step and 0.3 mm rising transition to the outer shell (magnification in Fig. 1). Subsequently, superimposition was performed with the samples using an initial-fit followed by a best-fit alignment which uses an iterative closest point algorithm. To determine the alingnment error of the software, superimposition procedure was repeated five time with each technology. For the best-fit superimposition, areas where support structures were attached, pressure artefacts and fractured edge areas were excluded from the superimposition. The three-dimensional surface comparison was performed separately for the three segments. The previously excluded areas were also not included in the evaluation.

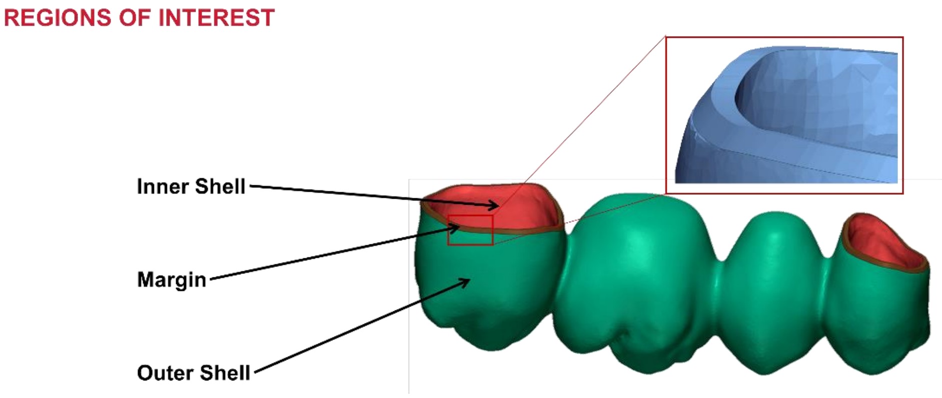

Fig. 1: Image of the regions of interest represented by the inner shell, margin and outer shell of the four-unit fixed dental prostheses.

2.4. Statistical analysis

The statistical evaluation of the surface deviation was performed using the root mean square error (RMSE) method, and the descriptive evaluation of the deviations was performed using the positive and negative mean surface deviation. The data were first tested for normal distribution using Shapiro-Wilk test. Subsequently, a nonparametric Kurskal-Wallis test with post hoc Wilcoxon-Mann-Whitney U test was performed. Significance values have been adjusted by the Bonferroni correction for multiple tests. The statistical analysis was carried out with an established software program (IBM SPSS Statistics, v24.0; IBM Corp) ($\alpha = 0.05$).

3. Results

Fig. 2 shows examples of zirconia FDPs produced according to the STL-file (Fig. 2a) by means of additive (Fig. 2b) and subtractive (Fig. 2c) manufacturing.

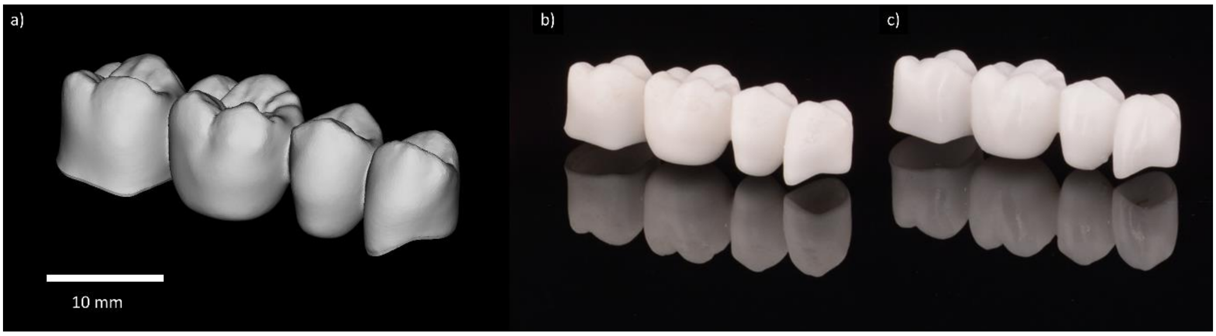

Fig. 2: a) STL of a four-unit zirconia fixed dental prostheses, b) example of an additively manufactured (aMJ) FDP , c) FDP produced by subtractive manufacturing.

The different digitalization techniques showed different deviations. The optical 3D coordinate measuring machine showed a positive mean deviation of 21 µm and a negative mean deviation of -18 µm. Only 78 % of the data points were within the tolerance of 20 µm. With the non-contact 3D profilometer, due to the stationary positioning during the measurement, data acquisition in undercut areas was difficult. Confocal laser scanning had a mean deviation of ±12 µm with 95 % of the data points within the tolerance of 20 µm. With a positive mean deviation of 7 µm and negative mean deviation of -6 µm, dynamic depth scanning showed the highest repeatability. Across the five scans, 98% of all data points were within a tolerance of 20 µm. Dynamic depth scanning was therefore used for digitizing the FDPs. The determination of the alignment error for the software Geomagic Control X did not result in measureable different values for the superimposition of the STLs.

Heat maps comparing the measured data with the CAD file of the samples manufactured with the different technologies are shown in Fig. 3.

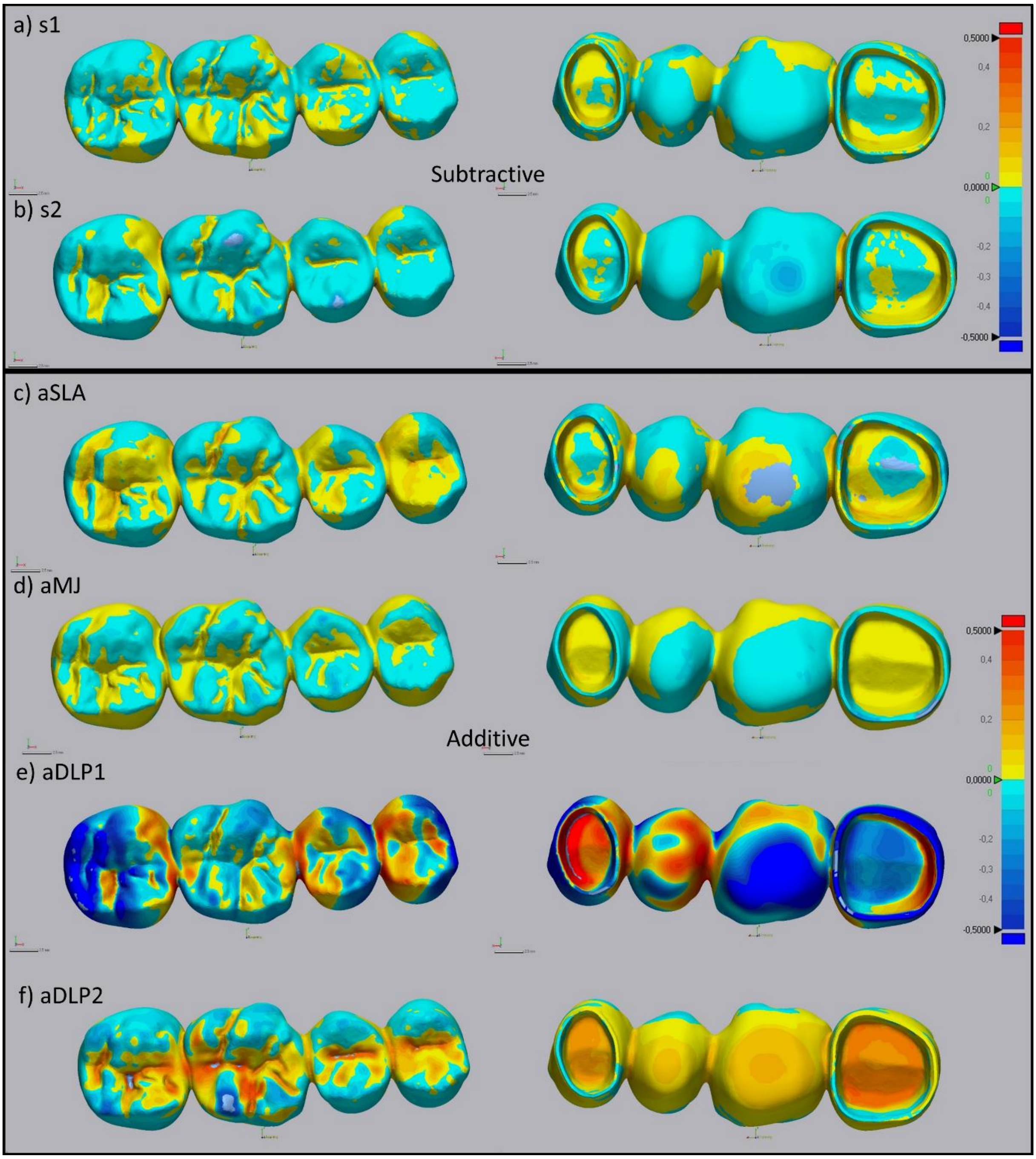

Fig. 3: Representative heat maps visualizing the deviation of the scanned samples compared to the CAD file. a)-b) subtractive (s1 and s2), c) stereolithography (aSLA), d) material jetting (aMJ), e)-f) digital light processing (aDLP1 and aDLP2). Yellow and red colored surfaces represent areas with a positive deviation (excess material). Blue color shows a negative deviation and therefore a lack of material.

The root mean square error of the samples produced with the different manufacturing technologies is shown in Table 2 and visualized in Fig. 4 for the outer shell, the margin, and the inner shell.

Table 2: RMSE of different ROI.

	RMSE (µm)		
	Outer Shell	Inner Shell	Margin
s1	27 ± 4	28 ± 6	27 ± 6
s2	44 ± 7	40 ± 8	49 ± 15
aSLA	73 ± 16	68 ± 8	70 ± 46
aMJ	46 ± 17	53 ± 19	125 ± 109
aDLP1	243 ± 26	288 ± 48	389 ± 80
aDLP2	108 ± 15	141 ± 7	67 ± 40

Detailed positive and negative mean surface deviations are presented in Fig. 5 and Fig. 6.

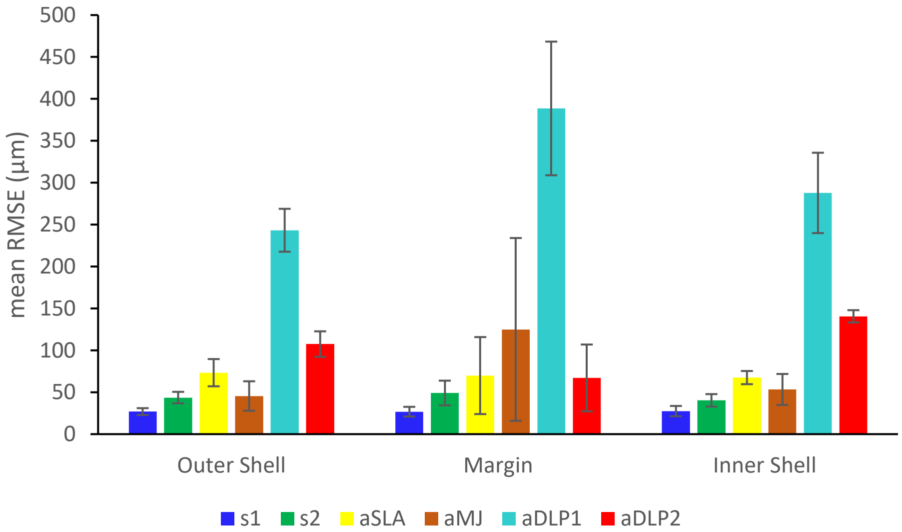

Fig. 4: Root mean square error (RMSE) of the samples produced with different manufacturing technologies for the outer shell, margin and inner shell.

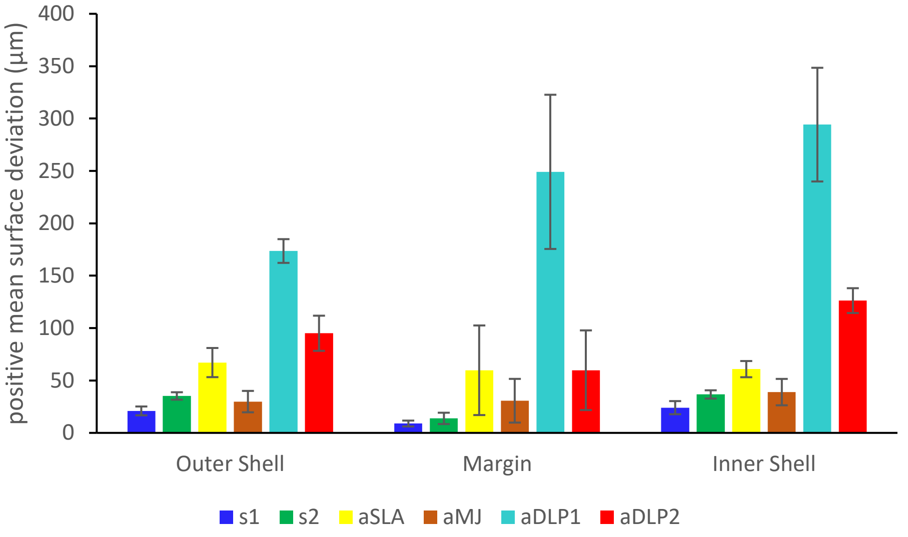

Fig. 5: Positive mean surface deviation from the STL file of the samples produced with different manufacturing technologies for the outer shell, margin and inner shell.

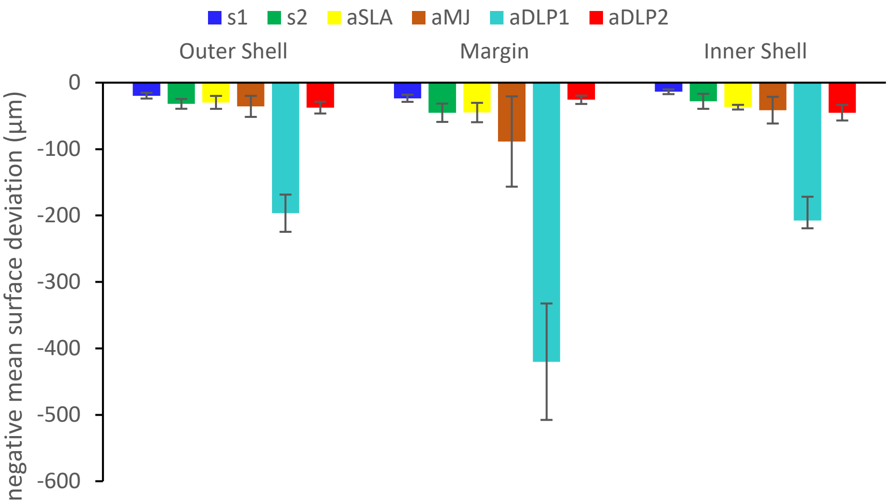

Fig. 6: Negative mean surface deviation from the STL file of the samples produced with different manufacturing technologies for the outer shell, margin and inner shell.

3.1. Inner Shell

Kruskal-Wallis test revealed significant differences in RMSE between groups ($P < 0.001$). The smallest differences were shown by s1 with no significant difference from s2 ($P = 0.297$). Compared with s2, aMJ ($P > 0.999$) and aSLA ($P = 0.085$) showed no statistically significant differences. aDLP1 showed significantly higher deviations than the other groups ($P < 0.001$). The negative mean deviations of all groups were smaller than the positive mean deviations. Only aDLP2 and aDLP1 showed mean surface deviation > 100 µm. All others showed mean deviations of < 50 µm for the positive and negative mean surface deviation, except for aSLA with < 100 µm for the positive mean surface deviation.

3.2. Margin

RMSE shows significant differences between the groups ($P < 0.001$). Congruent with inner shell, s1 showed the least deviation with no significant difference from s2 ($P = 0.097$), and s2 did not differ from aMJ ($P = 0.274$) and aSLA ($P > 0.999$). The highest deviations were shown by aDLP1 ($P \leq 0.080$). The pMean was < 50 µm for s1, s2, and aMJ and < 100 µm for aSLA and aDLP2. The negative mean surface deviation was < 50 µm for all groups. Only aDLP1 showed higher mean surface deviations.

3.3. Outer shell

RMSE shows significant differences between the groups ($P < 0.001$). The smallest deviations were shown by group s1 without significant difference to group s2 ($P = 0.054$) and aMJ ($P = 0.121$). aSLA showed larger deviations that did not reach the significance level to s2 and aMJ ($P \geq 0.103$). Again, aDLP1 showed the largest deviations. The positive mean surface deviation was < 50 µm for s1, s2, aMJ, and < 100 µm for aSLA and aDLP2. The negative mean surface deviation was < 50 µm for all groups. Only aDLP1 showed higher mean surface deviations.

4. Discussion

4.1. Main findings

In this study, the accuracy of 3Y-TZP four-unit FDPs produced by additive manufacturing was analyzed. Subtractively manufactured 3Y-TZP FDPs (s1 and s2) served as reference samples. Additive manufacturing included three different vat photopolymerization processes (aSLA, aDLP1 and aDLP2) and one material jetting technology (aMJ). The analysis was conducted as a three-dimensional target/actual comparison based on the RMSE segmented into the three areas: inner shell, margin, and outer shell. The two subtractive processes showed the lowest deviations, followed by the MJ process and the SLA process. aDLP2 was only described descriptively due to the low number of samples but showed larger deviations than the previous groups. Samples of the group aDLP1 had the highest deviations, nearly twice as large as the other groups. This indicates that, regarding the accuracy, state-of-the-art subtractive manufacturing processes for fixed dental prostheses can still be considered superior to additive manufacturing.

4.2. Methodology

4.2.1. Sample preparation

Dental ceramics made from 3Y-TZP are currently mostly produced by CAD/CAM milling or grinding depending on the sintering stage [22]. This technique has been continuously improved over the past decades and provides reliable, strong FDPs [23]. Even though the subtractive manufacturing route is currently most used, AM of dental ceramics is drawing a lot of interest. Ceramic AM companies have started developing SLA and DLP printers focused on printing ceramics for dental applications. SLA and DLP has been used to accurately manufacture dental crowns and bridges [17, 18, 24-26]. Another popular and highly accurate AM technique for producing 3Y-TZP is material jetting, also known as inkjet printing. MJ allows to build up highly dense and accurate green bodies, speeding up the postprocessing route due to the limited amount of binder that has to be removed compared to SLA [27]. High strength 3Y-TZP ceramics have been reported to be obtained by MJ when printing in the preferable 0° direction [16, 28-30]. 3Y-TZP 3D-printed dental crowns have been produced, demonstrating the possibility to create accurate restorations using material jetting [29].

4.2.2. Measurement method

Studies on the accuracy of manufactured FDPs can be divided into two-dimensional and three-dimensional methods. In two-dimensional measurements, distances between two lines are measured. This can be done non-destructively by an impression replica technique using a silicone material and subsequently measuring the cross-sections, or destructively by cementing the FDPs, forming cross-sections and measuring the width of the cement gap afterwards. Three-dimensional methods include the measurement of the cement gap after taking X-Ray Tomography (µCT) images of the FDPs and using three-dimensional target/actual comparisons. Compared to measurements of the cement gap, the latter has the disadvantage that a clinically relevant fit is not determined. On the other hand, it is advantageous that the entire object surface is analyzed and three-dimensional shrinkage and distortion can be displayed by means of heat maps which is suitable for exploratory analyses.

Sample digitalization methods determine the methodical error in digital accuracy analysis. The gold standard was a long time represented by coordinate measuring machines based on tactile measuring technologies while nowadays also optical technologies are comparable with the advantage of 360° measurements. The use of an optical 3D coordinate measuring machine and a 3D profilometer were evaluated in preliminary tests, but intraoral scanning using the dynamic depth scanning technology showed the highest repeatability. This can be explained by the possibility of non-stop 360° scanning of the object, when using the mobile scanner. Using the other mentioned technologies for optical scanning, separate data sets of the inner and outer shells needed to be assembled by the software, resulting in a negative impact on repeatability. A three-dimensional surface comparison was chosen as the method for analysis. This allows the entire object surface to be analyzed and the level of deviations to be visualized as heat maps.

When comparing the STLs, reproducible alignment needs to be performed. O'Toole et al. [31] investigated different alignment procedures using the software Geomagic Control X. The least accurate alingement for an arbitrary defect showed an error of 139 µm (landmark alignment) and the best alignment still had a mathematical error of 22 µm (reference best-fit alignment). Our samples did not show any measureable different values for the superimposition in the software Geomagic Control X. This could be due to the different nature of the defect. O'Toole examined an artificial defect by removing a 300 µm layer of the occlusal surface, while in our case the whole scanned FDP deviated from the original STL due to the manufacturing process and we used the occlusal surface for the initial alignment. The results indicate that this method can be used to investigate accuracy and is suitable for comparing relative differences between groups, but still needs to be considered as an exploratory analysis. Comparable studies to this work did not evaluate the accuracy of the FDPs but derived it from the fit in predominantly two-dimensional measurements [17]. This was mostly evaluated by relining with silicone materials and sectioning or destructive analysis based on the width of the cement gap in cross-sections. An alternative would have been the digitization method using a µCT. However, the mean surface deviations of < 7 µm on repeated scans were considered clinically sufficient.

A risk of bias of the present study might be seen in the manual exclusion of artifacts and support structures during evaluation. Since the focus was on warpage and shrinkage, these were excluded so that isolated partially operator-dependent areas would not affect the results.

4.3. Subtractive vs additive manufacturing technologies in relation to clinical needs

CAD-CAM fabrication of multi-span fixed restorations has been extensively studied, still the standard for a minimum accuracy requirement in ceramic dentistry is not yet defined [32]. In a systematic review, Hasanzade et al. [33] investigated digital and conventional fabrication methods for the fabrication of FDPs, with the tendency for the best internal and marginal fit being achieved with a fully digital workflow. However, this included only subtractive procedures. The clinical relevance of the deviations depends on the region and its influence on the fit. It is generally accepted that a marginal gap width smaller than 120 µm is clinically acceptable [34]. Overall in the entire internal and marginal fit of the FDP, a maximal deviation of 100 µm is reported as the limit to be considered clinically acceptable [35, 36]. The external accuracy is influenced by final machining and polishing, but should be as low as possible in a model-free production in order not to negatively influence the occlusion. The final fit of the FDP will be determined by its accuracy, which depends strongly on the fabrication process [17, 18, 26]. Poor accuracy and the concomitant poor fit result in a higher risk of plaque accumulation, inflammation and reduced strength of the FDP [37, 38].

The two subtractively fabricated groups (s1 and s2) showed the lowest deviations in this study with mean deviations smaller than 50 µm in all areas, which is in accordance with earlier studies that reported marginal discrepancy of 17 to 118 µm [26, 39-53] for milled zirconia bridges. Furthermore, there is no significant difference between the FDPs s1 (GC) and s2 (Pritidenta) ($p>0.096$). Both these results indicate the high quality of the subtractively produced FDPs.

The additive manufactured groups showed deviations in accordance to the maturity degree of the technology. While the samples produced by commercially available systems (aSLA, aMJ, aDLP2) had mean negative deviations of -88 µm and mean positive deviations +126 µm, the prototype DLP-Printer (aDLP1) revealed the highest negative mean deviation of -420 µm and positive mean deviation of +294 µm. Although high-strength standard shaped disk and bars can be manufactured by the identical route used by aDLP1, the fabrication process and shrinkage adjustment to make complex shaped fixed dental prostheses needs to be tailored.

Several studies analyzed the trueness of vat polymerization (SLA and DLP) produced molar crowns, reporting that it was possible to produce crowns with highly accurate dimensions, but that the gap width was larger than what can be obtained by subtractive manufacturing and possibly not sufficient yet for clinical application [17]. The average deviation of a DLP printed implant was reported as 89 µm and −129 µm (± 68 µm) homogenously distributed along the length of the printed implant [54].

Alumina single crowns manufactured using aDLP2 were reported to show a dimensional accuracy of 41 ± 11 µm and zirconia single crowns manufactured by a SLA process had an accuracy of 65 ± 6 µm [18]. Both AM produced crowns had a higher accuracy than subtractive milled zirconia crowns (72 ±13 µm) which is explained by the higher precision of the laser and photodiode compared to subtractive methods [18]. The accuracy of the single crowns produced by vat polymerization was considered within clinically acceptable limits [18, 26].

One study reported most defects on the inner and the marginal area [17], whereas another reported occlusal grooves showed the highest positive deviations, caused by the layerwise buildup, having the highest influence on curved surfaces [26]. While it was possible to observe the layerwise buildup on the surface of our samples, similar to other studies [17, 18, 26], only minor differences in accuracy between outer shell, inner shell and margin were observed.

Multiple parameters influence the dimensional accuracy during manufacturing including layer thickness, degree of polymerization, excessive polymerization, polymerization and sintering shrinkage and staircase effect [55, 56]. In contrast to additive manufacturing of polymer materials, the accuracy of AM ceramics is not only affected by the printing technique, but also by the factors chosen for the manufacturing technique, like slurry composition, layer thickness, polymerization parameters as well as by the following downstream process steps such as cleaning, debinding and the shrinkage of the ceramic during sintering [18, 56]. When analyzing the accuracy of a DLP produced FDP green body, it was reported that both pits and protrusions resulted in the highest deviations due to support damage [24]. According to the authors, negative deviations at the axial surface and margin area could have been caused by inadequate compensation for sintering shrinkage [26]. Less deviation and shrinkage in restorations manufactured with DLP is reached for short-unit restorations [57]. Especially for 3D-printed ceramics, controlling the shrinkage and warping during sintering is more challenging for FDPs than for smaller parts like single cowns. For subtractively produced single crowns, RMSE of 52 ± 18 µm (outer shell), 43 ± 12 µm (inner shell) and 35 ± 7 µm (margin area) compared to a RMSE of crowns produced with aSLA of 53 ± 9 µm (outer shell), 38 ± 12 µm (inner shell) and 34 ± 5 µm (margin area) were reported [26]. For our subtractively manufactured four-unit fixed dental prostheses s1, RMSE of 27 ± 4 µm (outer shell), 28 ± 6 µm (inner shell) and 27 ± 6 µm (margin area) were estimated. For FDPs s2, RMSE of 44 ± 7 µm (outer shell), 40 ± 8 µm (inner shell) and 49 ± 15 µm (margin area) was measured. The higher RSME found in our aSLA FDPs of 73 ± 16 µm (outer shell), 68 ± 8 µm (inner shell) and 69 ± 46 µm (margin area) shows the challenge for processing highly accurate long-span dental restaurations, like the investigated four-unit FDPs.

Subtractive manufacturing uses prefabricated blanks which ensure a homogenous powder compact. This leads to a controllable shrinkage and high predictability of the FDP dimensional changes during sintering. On the other hand, the homogeneity of the printed green body can be disturbed, e.g. by the layered structure leading to anisotropic shrinkage during sintering [20, 58]. This can negatively influence the predictability and the final accuracy of the 3D-printed components.

aMJ has shown the best results among the studied AM FDPs for the inner and outer shell, with results close to the subtractive manufactured FDPs and no significant differences to s2. Due to the lower layer thickness (10.5 μm compared to 25 μm) and the high green body density, this technique allows for the production of parts showing trueness comparable to conventional manufacturing, within the clinically acceptable limit of <100 μm. The margin area of aMJ FDPs shows a higher deviation because the thin restoration margins tended to break during the support removal in water, leading to higher negative deviations. It has been reported that it is possible to acquire highly accurate designs using the XJET printer, but that the printing of complex designs with fine features, like a thin restoration margin, are still challenging due to the support removal [16, 59].

4.4. Challenges to be overcome and perspectives

Subtractive manufacturing in dentistry has evolved over the past decades into a mature technology resulting in precisely adjusted manufacturing systems and processing parameters. AM of ceramics for dental applications is an emerging technology combininig many processing parameters that still need to be tailored. Especially the control of shrinkage behavior is important to obtain accurate final restorations [17]. Intensive research on improving the additive manufacturing methods, devices and material is still necessary to obtain high quality dental materials [60].

At the moment, AM of ceramics is a time-demanding manufacturing process. Grinding of the s1 fixed dental prostheses was performed in 30 min. Sintering of milled restorations takes, according to manufacturer recommendation approx. 7 h, but can be reduced to approx. 90 min with state of the art high-speed sintering cycle proposed for single crowns and 3-unit fixed dental prostheses restorations [61, 62]. New research shows that high-speed sintering in just 30 min, including cooling time, is possible [63]. However, 3D printing is much more time demanding. In systems like DLP or SLA, the polymer matrix needs to be thermally removed in a debinding step. The steps of drying and debinding can take more than 20 hours for smaller cylindrical parts with 4 mm in diameter [64]. In this work, more than four days of debinding were applied to aSLA FDPs. Debinding and sintering of alumina crowns fabricated with aDLP2 was reported to take 200 h [18].

Furthermore, the ceramic green bodies produced by AM are often handled manually during subsequent post-processing, which has a higher risk of introducing new defects, which also increases the cost of the additive manufacturing process [19, 21]. Therefore, further development is needed to reach the productivity of modern subtractive manufacturing systems and additional investigations for the reliability of the produced parts for long-term use are necessary.

5. Conclusion

Significant differences were calculated between the different subtractive and additive manufacturing technologies ($p<0.001$) used for preparing zirconia FDPs. The two subtractive groups were the most accurate with no significant difference regarding the used material or device (s1/s2, $p>0.054$). Likewise, no statistical difference regarding accurary was found when comparing the subtractive group s2 with the additive manufactured FDPs, aMJ and aSLA, in most ROIs ($p>0.085$). In general, mean surface deviation was <50 µm for s1, s2 and aMJ and <100 µm for aSLA and aDLP2. aDLP1 showed surface devitions >100 µm and was the least accurate method, compared to the other additive/subtractive technologies.

References

[1] Revilla-León M, Özcan M. Additive Manufacturing Technologies Used for Processing Polymers: Current Status and Potential Application in Prosthetic Dentistry. Journal of Prosthodontics. 2019;28:146-58.
[2] Revilla-León M, Sadeghpour M, Özcan M. A Review of the Applications of Additive Manufacturing Technologies Used to Fabricate Metals in Implant Dentistry. Journal of Prosthodontics. 2020;29:579-93.
[3] Denry I, Holloway JA. Ceramics for Dental Applications: A Review. Materials. 2010;3:351-68.
[4] Grech J, Antunes E. Zirconia in dental prosthetics: A literature review. Journal of Materials Research and Technology. 2019;8:4956-64.
[5] Guazzato M, Albakry M, Ringer SP, Swain MV. Strength, fracture toughness and microstructure of a selection of all-ceramic materials. Part II. Zirconia-based dental ceramics. Dental Materials. 2004;20:449-56.
[6] Hannink RHJ, Kelly PM, Muddle BC. Transformation Toughening in Zirconia-Containing Ceramics. Journal of the American Ceramic Society. 2000;83:461-87.
[7] Chen Z, Li Z, Li J, Liu C, Lao C, Fu Y, et al. 3D printing of ceramics: A review. Journal of the European Ceramic Society. 2019;39:661-87.
[8] Li H, Song L, Sun J, Ma J, Shen Z. Dental ceramic prostheses by stereolithography-based additive manufacturing: potentials and challenges. Advances in Applied Ceramics. 2019;118:30-6.

[9] Oh Y, Bharambe V, Mummareddy B, Martin J, McKnight J, Abraham MA, et al. Microwave dielectric properties of zirconia fabricated using NanoParticle Jetting™. Additive Manufacturing. 2019;27:586-94.
[10] XJet. XJet & NanoParticle jetting Technology.
[11] Felton DA, Kanoy BE, Bayne SC, Wirthman GP. Effect of in vivo crown margin discrepancies on periodontal health. J Prosthet Dent. 1991;65:357-64.
[12] Hunter AJ, Hunter AR. Gingival margins for crowns: a review and discussion. Part II: Discrepancies and configurations. J Prosthet Dent. 1990;64:636-42.
[13] Rekow ED, Harsono M, Janal M, Thompson VP, Zhang G. Factorial analysis of variables influencing stress in all-ceramic crowns. Dental Materials. 2006;22:125-32.
[14] Tuntiprawon M, Wilson PR. The effect of cement thickness on the fracture strength of all-ceramic crowns. Australian Dental Journal. 1995;40:17-21.
[15] Sun J, Chen X, Wade-Zhu J, Binner J, Bai J. A comprehensive study of dense zirconia components fabricated by additive manufacturing. Additive Manufacturing. 2021;43:101994.
[16] Willems E, Turon-Vinas M, Camargo dos Santos B, Van Hooreweder B, Zhang F, Van Meerbeek B, et al. Additive manufacturing of zirconia ceramics by material jetting. Journal of the European Ceramic Society. 2021;41:5292-306.
[17] Revilla-León M, Methani MM, Morton D, Zandinejad A. Internal and marginal discrepancies associated with stereolithography (SLA) additively manufactured zirconia crowns. The Journal of Prosthetic Dentistry. 2020;124:730-7.
[18] Wang W, Sun J. Dimensional accuracy and clinical adaptation of ceramic crowns fabricated with the stereolithography technique. The Journal of Prosthetic Dentistry. 2021;125:657-63.
[19] Harrer W, Schwentenwein M, Lube T, Danzer R. Fractography of zirconia-specimens made using additive manufacturing (LCM) technology. Journal of the European Ceramic Society. 2017;37:4331-8.
[20] Suominen JM, Frankberg EJ, Vallittu PK, Levänen E, Vihinen J, Vastamäki T, et al. Three-dimensional printing of zirconia: characterization of early stage material properties. Biomaterial Investigations in Dentistry. 2019;6:23-31.
[21] Saâdaoui M, Khaldoun F, Adrien J, Reveron H, Chevalier J. X-ray tomography of additive-manufactured zirconia: Processing defects – Strength relations. Journal of the European Ceramic Society. 2020;40:3200-7.
[22] Galante R, Figueiredo-Pina CG, Serro AP. Additive manufacturing of ceramics for dental applications: A review. Dental Materials. 2019;35:825-46.
[23] Miyazaki T, Nakamura T, Matsumura H, Ban S, Kobayashi T. Current status of zirconia restoration. Journal of Prosthodontic Research. 2013;57:236-61.
[24] Lian Q, Wu X, Li D, He X, Meng J, Liu X, et al. Accurate printing of a zirconia molar crown bridge using three-part auxiliary supports and ceramic mask projection stereolithography. Ceramics International. 2019;45:18814-22.
[25] Ioannidis A, Bomze D, Hämmerle CHF, Hüsler J, Birrer O, Mühlemann S. Load-bearing capacity of CAD/CAM 3D-printed zirconia, CAD/CAM milled zirconia, and heat-pressed lithium disilicate ultra-thin occlusal veneers on molars. Dental Materials. 2020;36:e109-e16.
[26] Wang W, Yu H, Liu Y, Jiang X, Gao B. Trueness analysis of zirconia crowns fabricated with 3-dimensional printing. The Journal of Prosthetic Dentistry. 2019;121:285-91.
[27] Özkol E, Ebert J, Uibel K, Wätjen AM, Telle R. Development of high solid content aqueous 3Y-TZP suspensions for direct inkjet printing using a thermal inkjet printer. Journal of the European Ceramic Society. 2009;29:403-9.
[28] Özkol E, Wätjen AM, Bermejo R, Deluca M, Ebert J, Danzer R, et al. Mechanical characterisation of miniaturised direct inkjet printed 3Y-TZP specimens for microelectronic applications. Journal of the European Ceramic Society. 2010;30:3145-52.

[29] Ebert J, Özkol E, Zeichner A, Uibel K, Weiss Ö, Koops U, et al. Direct Inkjet Printing of Dental Prostheses Made of Zirconia. Journal of Dental Research. 2009;88:673-6.
[30] Özkol E, Zhang W, Ebert J, Telle R. Potentials of the "Direct inkjet printing" method for manufacturing 3Y-TZP based dental restorations. Journal of the European Ceramic Society. 2012;32:2193-201.
[31] O'Toole S, Osnes C, Bartlett D, Keeling A. Investigation into the accuracy and measurement methods of sequential 3D dental scan alignment. Dental Materials. 2019;35:495-500.
[32] ISO. ISO 6872: 2015 Dentistry - Ceramic materials. ISO; 2015. p. 28.
[33] Hasanzade M, Aminikhah M, Afrashtehfar KI, Alikhasi M. Marginal and internal adaptation of single crowns and fixed dental prostheses by using digital and conventional workflows: A systematic review and meta-analysis. The Journal of Prosthetic Dentistry. 2020.
[34] McLean JW, von F. The estimation of cement film thickness by an in vivo technique. British Dental Journal. 1971;131:107-11.
[35] Rungrojwittayakul O, Kan JY, Shiozaki K, Swamidass RS, Goodacre BJ, Goodacre CJ, et al. Accuracy of 3D Printed Models Created by Two Technologies of Printers with Different Designs of Model Base. Journal of Prosthodontics. 2020;29:124-8.
[36] Daou EE, Ounsi H, Özcan M, Al-Haj Husain N, Salameh Z. Marginal and internal fit of pre-sintered Co-Cr and zirconia 3-unit fixed dental prostheses as measured using microcomputed tomography. The Journal of Prosthetic Dentistry. 2018;120:409-14.
[37] Schriwer C, Skjold A, Gjerdet NR, Øilo M. Monolithic zirconia dental crowns. Internal fit, margin quality, fracture mode and load at fracture. Dental Materials. 2017;33:1012-20.
[38] Knoernschild KL, Campbell SD. Periodontal tissue responses after insertion of artificial crowns and fixed partial dentures. The Journal of Prosthetic Dentistry. 2000;84:492-8.
[39] Sulaiman F, Chai J, Jameson L, Wozniak W. A comparison of the marginal fit of In-Ceram, IPS Empress, and Procera crowns. The International journal of prosthodontics. 1997;10 5:478-84.
[40] Lee K-B, Park C-W, Kim K-H, Kwon T-Y. Marginal and Internal Fit of All-ceramic Crowns Fabricated with Two Different CAD/CAM Systems. Dental Materials Journal. 2008;27:422-6.
[41] Baig MR, Tan KB-C, Nicholls JI. Evaluation of the marginal fit of a zirconia ceramic computer-aided machined (CAM) crown system. The Journal of Prosthetic Dentistry. 2010;104:216-27.
[42] Grenade C, Mainjot A, Vanheusden A. Fit of single tooth zirconia copings: comparison between various manufacturing processes. The Journal of Prosthetic Dentistry. 2011;105:249-55.
[43] Karatasli, Ouml, zge, Kursoglu P, Ccedil, Apa N, et al. Comparison of the marginal fit of different coping materials and designs produced by computer aided manufacturing systems. Dental Materials Journal. 2011;30:97-102.
[44] Rinke S, Fornefett D, Gersdorff N, Lange K, Roediger M. Multifactorial analysis of the impact of different manufacturing processes on the marginal fit of zirconia copings. Dental Materials Journal. 2012;31:601-9.
[45] Coli P, Karlsson S. Precision of a CAD/CAM technique for the production of zirconium dioxide copings. Int J Prosthodont. 2004;17:577-80.
[46] May KB, Russell MM, Razzoog ME, Lang BR. Precision of fit: The Procera AllCeram crown. The Journal of Prosthetic Dentistry. 1998;80:394-404.
[47] Beschnidt SM, Strub JR. Evaluation of the marginal accuracy of different all-ceramic crown systems after simulation in the artificial mouth. J Oral Rehabil. 1999;26:582-93.
[48] Boening KW, Wolf BH, Schmidt AE, Kästner K, Walter MH. Clinical fit of Procera AllCeram crowns. The Journal of Prosthetic Dentistry. 2000;84:419-24.

[49] Yeo I-S, Yang J-H, Lee J-B. In vitro marginal fit of three all-ceramic crown systems. The Journal of Prosthetic Dentistry. 2003;90:459-64.
[50] Suárez MJ, González de Villaumbrosia P, Pradíes G, Lozano JF. Comparison of the marginal fit of Procera AllCeram crowns with two finish lines. Int J Prosthodont. 2003;16:229-32.
[51] Quintas AF, Oliveira F, Bottino MA. Vertical marginal discrepancy of ceramic copings with different ceramic materials, finish lines, and luting agents: an in vitro evaluation. The Journal of Prosthetic Dentistry. 2004;92:250-7.
[52] Balkaya MC, Cinar A, Pamuk S. Influence of firing cycles on the margin distortion of 3 all-ceramic crown systems. The Journal of Prosthetic Dentistry. 2005;93:346-55.
[53] Beuer F, Aggstaller H, Edelhoff D, Gernet W, Sorensen J. Marginal and internal fits of fixed dental prostheses zirconia retainers. Dental Materials. 2009;25:94-102.
[54] Osman RB, van der Veen AJ, Huiberts D, Wismeijer D, Alharbi N. 3D-printing zirconia implants; a dream or a reality? An in-vitro study evaluating the dimensional accuracy, surface topography and mechanical properties of printed zirconia implant and discs. Journal of the Mechanical Behavior of Biomedical Materials. 2017;75:521-8.
[55] Halloran JW. Ceramic Stereolithography: Additive Manufacturing for Ceramics by Photopolymerization. Annual Review of Materials Research. 2016;46:19-40.
[56] Tian X, Li D, Chen Z, Zhou W. Study on the fabrication accuracy of ceramic parts by direct stereolithography. Virtual and Physical Prototyping. 2012;7:195-202.
[57] Moon W, Kim S, Lim B-S, Park Y-S, Kim RJ-Y, Chung SH. Dimensional Accuracy Evaluation of Temporary Dental Restorations with Different 3D Printing Systems. Materials. 2021;14:1487.
[58] Manière C, Kerbart G, Harnois C, Marinel S. Modeling sintering anisotropy in ceramic stereolithography of silica. Acta Materialia. 2020;182:163-71.
[59] Mummareddy B, Negro D, Bharambe VT, Oh Y, Burden E, Ahlfors M, et al. Mechanical properties of material jetted zirconia complex geometries with hot isostatic pressing. Advances in Industrial and Manufacturing Engineering. 2021;3:100052.
[60] Liaw C-Y, Guvendiren M. Current and emerging applications of 3D printing in medicine. Biofabrication. 2017;9:024102.
[61] Noritake K. Katana Zirconia restoration systems.
[62] Kuraray N. Katanay Zirconia Technical Guide.
[63] Cokic SM, Vleugels J, Van Meerbeek B, Camargo B, Willems E, Li M, et al. Mechanical properties, aging stability and translucency of speed-sintered zirconia for chairside restorations. Dental Materials. 2020;36:959-72.
[64] Mitteramskogler G, Gmeiner R, Felzmann R, Gruber S, Hofstetter C, Stampfl J, et al. Light curing strategies for lithography-based additive manufacturing of customized ceramics. Additive Manufacturing. 2014;1-4:110-8.